Metabolic diversity conveyed by the process leading to glutathione accumulation in inactivated dry yeast: A synthetic media study

Florian Bahut, Youzhong Liu, Remy Romanet, Christian Coelho, Nathalie Sieczkowski, Hervé Alexandre, Philippe Schmitt-Kopplin, Maria Nikolantonaki, Régis Gougeon

▶ **To cite this version:**

Florian Bahut, Youzhong Liu, Remy Romanet, Christian Coelho, Nathalie Sieczkowski, et al.. Metabolic diversity conveyed by the process leading to glutathione accumulation in inactivated dry yeast: A synthetic media study. Food Research International, 2019, 123, pp.762-770. 10.1016/j.foodres.2019.06.008 . hal-02173718

HAL Id: hal-02173718

https://u-bourgogne.hal.science/hal-02173718

Submitted on 25 Oct 2021

HAL is a multi-disciplinary open access archive for the deposit and dissemination of scientific research documents, whether they are published or not. The documents may come from teaching and research institutions in France or abroad, or from public or private research centers.

L'archive ouverte pluridisciplinaire **HAL**, est destinée au dépôt et à la diffusion de documents scientifiques de niveau recherche, publiés ou non, émanant des établissements d'enseignement et de recherche français ou étrangers, des laboratoires publics ou privés.

Distributed under a Creative Commons Attribution - NonCommercial 4.0 International License

Version of Record: https://www.sciencedirect.com/science/article/pii/S0963996919303631
Manuscript_aac47afb34717451f7689e2100790754

Metabolic diversity conveyed by the process leading to glutathione accumulation in inactivated dry yeast: a synthetic media study

Florian BAHUT[a], Youzhong LIU[a], Rémy ROMANET[a], Christian COELHO[a], Nathalie SIECZKOWSKI[b], Hervé ALEXANDRE[a], Philippe SCHMITT-KOPPLIN[c,d], Maria NIKOLANTONAKI[a] and Régis D. GOUGEON[a*]

[a]*Univ. Bourgogne Franche-Comté, AgroSup Dijon, PAM UMR A 02.102, Institut Universitaire de la Vigne et du Vin – Jules Guyot, F-21000 Dijon, France*

[b]*Lallemand SAS, 19 rue des Briquetiers, BP 59, 31 702 Blagnac, France*

[c]*Research Unit Analytical BioGeoChemistry, Helmholtz Zentrum Muenchen, 85764 Neuherberg, Germany*

[d]*Technische Universität München, Analytical Food Chemistry, Alte Akademie 10, 85354 Freising, Germany*

Corresponding Author

*Université de Bourgogne, UMR PAM, 2 rue Claude Ladrey, 21000 Dijon, France. Email: regis.gougeon@u-bourgogne.fr

© 2019 published by Elsevier. This manuscript is made available under the CC BY NC user license
https://creativecommons.org/licenses/by-nc/4.0/

ABSTRACT

Glutathione-rich inactivated dry yeasts (GSH-IDY) are purported to accumulate glutathione intracellularly and then released into the must. Glutathione is beneficial for wine quality, but research has highlighted that GSH-IDYs have a synergic antioxidant effect similar to that of molecular GSH. Combination of negative mode ultra-high-resolution Fourrier-Transform Ion-Cyclotron-Resonance Mass Spectrometry ((-)FT-ICR-MS), ultra-high-performance liquid chromatography coupled to a Quadrupole-Time of Flight mass spectrometer (UHPLC-Q-ToF-MS) and HPLC/Diode Detector Array (DAD)-Fluorescence spectroscopy was applied to three inactivated dry yeasts soluble fractions, with increasing intracellular glutathione concentration, in order to explore the chemical diversity released in different synthetic media.

Using the mean of size exclusion chromatography/DAD and fluorescence detection we report than most of the signals detected were below the 5-75 kDa-calibrated region of the chromatogram, indicating that most of the soluble protein fraction is composed of low molecular weight soluble peptides. In light of these results, high-resolution mass spectrometry was used to scan and annotate the low molecular weight compounds from 50 to 1500 Da and showed that GSH level of enrichment in IDYs was correlated to a discriminant chemical diversity of the corresponding soluble fractions. Our results clearly show an impact of the GSH accumulation process not only visible on the glutathione itself, but also on the global diversity of compounds. Within the 1674 ions detected by (-)FT-ICR-MS, the ratio of annotated elemental formulas containing carbon, hydrogen, oxygen, nitrogen and sulphur (CHONS) to annotated elemental formulas containing carbon, hydrogen, oxygen (CHO) increased from 0.2 to 2.1 with the increasing levels of IDYs GSH content and 36 unique CHONS annotated formulas were unique to the IDY with the highest concentration of GSH. Amongst the 1674 detected ions 193 were annotated as potential peptides (from 2 to 5

residues), 61 ions were annotated as unique amino acid combinations and 46% of which being significantly more intense in GSH-rich IDY. Thus, the process leading to the accumulation of glutathione also involves other metabolic pathways which contribute to an increase in CHONS containing compounds potentially released in wine, notably peptides.

KEYWORDS: Mass spectrometry; Wine; Oenology; Untargeted analysis

CHEMICAL COMPOUNDS STUDIED IN THIS ARTICLE

Glutathione (PubChem CID: 124886); Leucyl-arginine (PubChem CID: 3800205); Leucyl-lysine (PubChem CID: 14299197); Adenosine (PubChem CID: 60961); Glutamyl-cysteine (PubChem CID: 123938); Pantothenic acid (PubChem CID: 6613); Cysteinyl-glycine (PubChem CID: 439498); Pipecolic acid (PubChem CID: 439227); Homocitric acid (PubChem CID: 5460287); Methyl-thioadenosine (PubChem CID: 439176)

1. Introduction

There has been a growing interest for yeast derivatives in winemaking over the last few decades, as these products can improve fermentation processes and organoleptic properties of wine (recently reviewed by Pozo-Bayòn and collaborators (2009)). They divided enological preparations of yeast derivatives into five classes depending on the industrial process of production : the yeast hulls, yeast mannoproteins, the yeast autolysate, the yeast protein extracts and the inactivated dry yeasts (IDY). The latter are mainly *Saccharomyces cerevisiae* strains grown under aerobic condition in a non-limiting medium before being inactivated and dried and can then be used from the vineyards through to the fermentation and barrel aging steps of the winemaking process.

Although IDY have already been largely used in wineries, scientific explanations for their impact on winemaking have only recently been elucidated. IDY can release amino acids and peptides expressed in yeast assimilable nitrogen (of the order of a few mg N/L) which contribute to enrich the must in nutrients (Pozo-Bayón et al., 2009). Since the amount of nitrogen released by inactivated yeast is low (compared to yeast autolysates), these products are more generally advised for micronutrient and survival factors (notably vitamins and fatty acids). However, the extent of the fraction of assimilable nitrogen related to the presence of small peptides and proteins released by both active and IDY is still unexplored (Liu et al., 2017). Polysaccharides are also significantly released by IDY (Pozo-Bayón et al., 2009). The main component of the yeast cell wall is mannan (chains of mannose) and β-glucan (chains of glucose) which could be linked to proteins. Cell wall polysaccharides mainly have color stabilization properties (Escot et al., 2001; Guadalupe & Ayestarán, 2008), notably through polyphenolic interactions (Andújar-Ortiz et al., 2012). It is however acknowledged that cell walls can exhibit a potential antioxidant activity not only due to the linked proteins but also due to the polysaccharides structures themselves (Jaehrig et al., 2008; Jaehrig & Rohn, 2007).

Recently there has been an interest in the use IDYs during winemaking, notably with a focus on their antioxidant properties. The concept of IDY rich in glutathione (GSH), as natural antioxidant for a use in winemaking originated in 2005 with the first patent for naturally rich inactive yeast (PCT/FR2005/000115). Glutathione is a cysteine-containing peptide and is considered to be the most abundant low molecular thiol in yeast cells (Elskens et al., 1991). In winemaking, GSH has been proposed to reduce the oxidation phenomena that leads to browning, and thus improves wine preservation and varietal aroma stability during aging (Antoce et al., 2016; Kritzinger et al., 2013; Nikolantonaki et al., 2018; Webber et al., 2016).

IDY can have a higher GSH content by activating the GSH yeast intracellular production during processing (Li et al., 2004; Wen et al., 2004). The increase in GSH content of IDYs during processing can be achieved after modulation of the sulfur metabolic pathway when cysteine is present in the culture medium (Nisamedtinov et al., 2011). However, it is well known that sulfur-containing compounds can exert an antioxidant activity and these reactive compounds are more abundant in GSH-enriched IDY than in IDY (Elias et al., 2008; Rodriguez-Bencomo et al., 2014). Even though there is quite a lot of literature on the general metabolites which could impact the wine quality and safety, there is a lack of knowledge on the global diversity and functionality of IDY compounds released during winemaking and their impact on wines composition (Liu et al., 2016; Liu et al., 2017).

In this study, we combined various non-targeted analyses in order to characterize the diversity of compounds, which can be potentially extracted from GSH-enriched inactivated dry yeasts when added to wines. Three IDYs with increasing GSH enrichments were characterized for their potential molecular and macromolecular release, and the diversity of the annotated/identified compounds provides new insights on IDY functionalities under winemaking conditions, and underlines crucial IDY compositional differences in a GSH-accumulation process-dependent manner.

2. Material and methods

2.1. Sample preparation

Three non-commercial inactivated dry yeasts were obtained from Lallemand SAS (Blagnac, France). These products were produced at a laboratory scale process allowing optimizing chemical, physical and nutritional features of the bio-process in order to maximize the intracellular concentration of metabolites, notably glutathione. Two products were specifically produced from different yeast strains to increase the bioavailability of glutathione (G-IDY and Gplus-IDY which release 18 mg and 25 mg of glutathione per gram of IDY, respectively). The third product (N-IDY) was produced with the same strain as for G-IDY without following the specific process of GSH accumulation and releases 12 mg of glutathione per gram of IDY. At the first opening of the sealed prepared products, the three IDY products were aliquoted in pre-weighed 2 mL vials under nitrogen and stored at -18°C in dark. Three different extractions were made to obtain: the acidified Water-Soluble Fraction (WSF) from ultrapure water (18.2 MΩ, Millipore, Germany) with 0.01% (*v/v*) formic acid at pH 3.2, the Model Wine Soluble Fraction (MWSF), from 12% (*v/v*) ethanol in ultrapure water with 0.01% (*v/v*) formic acid at pH 3.2, and the Methanol Soluble Fraction (MSF), from methanol with 0.1% (*v/v*) formic acid. IDYs were resuspended at 4 g/L and soluble fractions were obtained after 1h stirring at room temperature in dark. Samples were then centrifuged (12000 g, 5 min, 4°C) and the supernatants were aliquoted and stored under nitrogen at 4°C until analysis. All samples were prepared in triplicate.

2.2. Gel Permeation Chromatography (GPC)

GPC was performed with a high-performance liquid chromatography (HPLC) (Elite LaChromElite, VWR, Radnor, Pennsylvanie) coupled to a Diode Array Detector (DAD)/Fluorescence detector. 50 µL of sample were injected through a column Yarra 3µ SEC-2000 300 x 7.8 mm (Phenomenex, Sartrouville, France) connected to a stationary phase

guard column with SecurityGuard (Phenomenex, Sartrouville, France). Elution was performed with hydro-alcoholic solution (12% *(v/v)* ethanol, 6 g/L of tartaric acid at pH 3.5) in an isocratic gradient (500 µL/min which corresponds to a pressure of 75 bars) for 45 min. The temperature of the sampler and the column were kept constant at 4°C and 25°C respectively during analysis. Fluorescence detector was set at 280 nm for the excitation wavelength and 350 nm for the emission wavelength, and the DAD enabled absorption spectra acquisition from 200 to 400 nm. Data were acquired with the EZChrom Elite (Agilent Technologies, Santa Clara, California) software, exported as .dat converted into .asc and processed with CHROMuLAN v0.79 (PiKRON Ltd.). Data were calibrated against a low molecular weight standards mix (LMW Gel Filtration calibration kits, GE Healthcare, Buckinghamshire) with the following standards: Conalbumin (75 kDa), Ovalbumin (43 kDa), Ribonuclease A (13.7 kDa), Aprotinin (6.5 kDa) and Angiotensine (1.1 kDa). Elution times were converted into molecular weight masses according to the calibration curve (Supplementary information 1).

2.3. Metabolomics analyses by Fourier Transform Ion Cyclotron Resonance Mass Spectrometry

Ultra-high-resolution mass spectra were acquired in negative mode on a Bruker SolariX Ion Cyclotron Resonance Fourier Transform Mass Spectrometer ((-)FT-ICR-MS) (BrukerDaltonics GmbH, Bremen, Germany) equipped with a 12 Tesla superconducting magnet (Magnex Scientific Inc., Yarnton, GB) and a APOLO II ESI source (BrukerDaltonics GmbH, Bremen, Germany), and operating in negative and positive ionization modes. 20 µL sample was diluted in 1mL of pure methanol and then injected at a flow rate of 120 µL/h into the microelectrospray. Spectra were acquired with a time-domain of 4 mega words over a mass range of *m/z* 147 to 2000. A total of 300 scans were accumulated for each sample. All samples were injected randomly in the same batch to avoid batch variability. External

157 calibration was done with clusters of arginine (10 mg/L in methanol). Internal calibration was
158 performed for each sample by using yeast ubiquitous compounds for negative mode
159 (Gougeon et al., 2009) (Supplementary information 2). External and internal calibration led to
160 a day-to-day mass accuracy lower than 0.1 ppm.

161 *2.4. Identification of metabolites by liquid chromatography coupled to time-of-flight mass*
162 *spectrometry*

163 Metabolite separation was performed with an ultra-high-performance liquid
164 chromatography (Dionex Ultimate 3000, ThermoFischer) coupled to a MaXis plus MQ ESI-
165 Q-ToF mass spectrometer (Bruker, Bremen, Germany). The non-polar and low polar
166 metabolites were separated in reversed phase liquid chromatography (RP-LC) by injecting
167 5 µL in an Acquity UPLC BEH C_{18} 1.7 µm column 100 x 2.1 mm (Waters, Guyancourt,
168 France). Elution was performed at 40°C by (A) acidified water with 0.1% (*v/v*) of formic acid
169 and (B) acetonitrile with 0.1% (*v/v*) of formic acid with the following gradient: 0-1.10 min 5%
170 (*v/v*) of B and 95% (*v/v*) of B at 6.40 min. The flow rate was set at 400 µL/min and
171 maintained for 5min at initial conditions before each injection. Solvent and analytes were
172 ionized with an electrospray (Nebulizer pressure = 2 bars and nitrogen dry gas flow = 10
173 L/min). Ions transfer was done with an end plate offset at 500 V and transfer capillary voltage
174 at 4500 V. A divert valve was used to inject four times diluted ESI-L Low Concentration
175 Tuning Mix (Agilent, Les Ulis, France) at the beginning of each run, allowing a recalibration
176 of each spectrum. The mass spectrometer was calibrated with undiluted Tuning Mix before
177 batch analysis in enhanced quadratic mode, with less than 0.5 ppm errors after calibration.
178 Spectra were acquired on the 100 to 1500 *m/z* mass range, both in negative and positive
179 ionization modes. UHPLC-Q-ToF-MS quality control (mix of standard peptides and
180 polyphenols) and experimental quality control (mix of samples) were used to guarantee the
181 UHPLC-Q-ToF-MS system performance. All samples were injected randomly in the same

batch to avoid batch-to-batch variability. Features (couple of *m/z*-values and retention times) fragmentation was performed using the AutoMS/MS function on the most intense features with a frequency of 2 Hz. The fragmentation was done at three different collision energies: 15, 25 and 35 eV.

2.5. Data analysis

Results were expressed as the average of three replicates with the associated standard deviations.

(-)FT-ICR-MS data were handled with DataAnalysis (v. 4.3, Bruker Daltonik GmbH). Calibrated data were filtered to keep only m/z peaks with a signal to noise (S/N) ratio above 10 and an absolute intensity higher than $2.0x10^6$. Peaks alignment was made by Matrix Generator software (v. 0.4, Helmholtz-Zentrum Muenchen) with a mass accuracy window of 1 ppm (Lucio, 2009). Peaks with intensity equal to 0 in more than 80% of samples were removed from the analysis. Finally, the in-house software NetCalc 2015 (v. 1.1a, Helmholtz-Zentrum Muenchen) was used to annotate peaks (Tziotis et al., 2011). 46% of the initially aligned peaks were annotated by NetCalc and used for this study. Van Krevelen diagrams, which plot the H/C against the O/C ratio of annotated metabolites were generated by an Excel file, providing instantaneous chemical pictures of the metabolites diversity (Brockman et al., 2018; Kim et al., 2003). The OligoNet webserver was also used to annotate potential peptides with a max error of 1 ppm (Liu et al., 2017).

The UHPLC-Q-ToF-MS data were calibrated internally by 1/4 diluted tuning mix with DataAnalysis (v. 4.3, Bruker Daltonik GmbH). Calibrated features were filtered to retain those with signal/noise ratio (S/N) higher than 30 and an absolute intensity of at least 1000. Before features extraction, the spectral background noise was removed. The extracted features were aligned with a R script with a *m/z* tolerance of 2 ppm and retention time tolerance of 0.2 seconds.

Parent ions and fragments were submitted to different databases with the MassTRIX interface (http://masstrix.org) (Suhre & Schmitt-Kopplin, 2008), Metlin (https://metlin.scripps.edu) and YMDB 2.0 (http://www.ymdb.ca) (Ramirez-Gaona et al., 2017). According to the precision of UHPLC-Q-ToF-MS and (-)FT-ICR-MS, an error of 3 ppm and 1 ppm was chosen respectively for the annotation of the metabolites (Roullier-Gall et al., 2014; Roullier-gall et al., 2015). The combination of these databases enabled covering the widest range of metabolites found in biological systems, and notably in yeast.

3. Results and discussion

3.1. IDY macromolecular profile

Besides the obvious discrimination between soluble and non-soluble fractions in a specific medium, the gel permeation chromatography is dedicated to determine the global size repartition of compounds within complex samples. This first experiment was a good introduction to understand the relatively unknown diversity of compounds released by IDY in different extraction media. Acidified water and model wine media were chosen to identify what can be released by IDY in must and wine, respectively. Methanol was used to have an overview of the mildly hydrophobic soluble fraction present in our samples, independent of the oenological conditions in winemaking process. In this experiment, it was possible to separate macromolecules from 300 kDa to 5 kDa between 9.5 min and 22.5 min depending on the column specification. Separation was performed with model wine and without any denaturant to keep macromolecules in their native forms. The fluorescent detector was set up to track the presence of potent proteinaceous fluorophores among the chromophore extracted from yeast extracts (Coelho et al., 2017). Figure 1 shows GPC chromatograms of MWSF for G-IDY, Gplus-IDY and N-IDY and supplementary information 3 shows those for WSF and MSF. These chromatograms clearly revealed three different time frame windows common to all MWSF extracts. The first time-frame (I) between 9.5 and 17.3 min (outside of the

232 calibrated region) represents about 1 % of the total fluorescent response and had a mass range
233 from 300 to 75 kDa. G-IDY, Gplus-IDY and N-IDY showed no significant differences in
234 abundance of high molecular weight molecules in this region. This result is in agreement with
235 Pozo-Bayon and collaborators (2009), who reported that high molecular weight compounds
236 are in lower concentration than peptides and amino acids in the model wine soluble fraction of
237 different IDY (Pozo-Bayón et al., 2009). Under our experimental conditions, the percentage
238 of high molecular weight compounds released from G-IDY, Gplus-IDY and N-IDY was
239 always low, whatever the solvent used (Supplementary information 3). However, methanol
240 extracts showed limited high molecular weight compounds response, probably because of
241 organic solvent precipitation (Chertov et al., 2004).

242 **FIGURE 1**

243

244 The second time-frame window (II) in the chromatogram, between 17.3 and 22.5 min,
245 represents medium molecular weight compounds in a mass range from 75 to 5 kDa, the latter
246 corresponding to the exclusion limit of the column. G-IDY, Gplus-IDY and N-IDY relative
247 concentrations in medium molecular weight compounds varied from 7 to 14% of the total
248 fluorescence of the sample, in an extraction medium dependent manner. In detail, WSF and
249 MWSF exhibited concentrations in medium molecular weight compounds, which were 1.5
250 times higher for Gplus-IDY compared to those for G-IDY and N-IDY. However, MSF
251 presented relatively low concentrations of medium molecular weight compounds, of about 3%
252 of the total fluorescence responses (Supplementary information 3).

253 Finally, the most abundant fluorescent responses (whatever the extraction media) were
254 observed for the third time-frame (III) from 22.5 to 45 min, where fluorescent compounds
255 accounted for 92%, 91% and 86% of the total fluorescence response of G-IDY, N-IDY, and
256 Gplus-IDY respectively in model wine extraction medium. This chromatographic region is

out of the molecular size exclusion limit of 5 kDa of the column and suggests the importance of low molecular weight compounds on the IDY soluble fraction independently of the extraction medium.

In addition, in order to get a more representative characterization of IDY soluble fractions, UV detection at 210 nm was also considered. UV detection is less sensitive and less specific compared to fluorescence, but allows the peptide bond, carbon to carbon and carbon to oxygen double bond detection (Stoscheck, 1990). Supplementary information 2 shows chromatograms of G-IDY, Gplus-IDY and N-IDY for the three extraction media, recorded at 210 nm. UV responses were far less important than those monitored with fluorescence, and concerned specifically the third time-domain corresponding to the low molecular weight compounds (below 5 kDa).

On the basis of these results, and whatever the detection method or the extraction medium used, GPC could not discriminate IDY soluble fractions. The medium and high molecular weight compounds showed a similar fluorescent profile among samples which indicated that the bio-process enrichment would only impact the low molecular weight fraction of IDYs. In that respect, to further the characterization of IDY soluble fractions, ultra-high-resolution mass spectrometry was used to assess the diversity of the abundant low molecular weight compounds.

3.2. IDY low molecular weight chemical diversity

The ultra-high accuracy of (-)FT-ICR-MS enables the exact mass of ionizable compounds present in complex matrices to be determined, including wine, thus allowing to have a more comprehensive picture of the chemical diversity present in the sample (Roullier-Gall et al., 2017, 2014). Figure 2A gives an overview of the number of ions detected in one specific IDY (G-IDY) in the three different extraction media. Within the 1280 ions detected

for G-IDY, 701 (54.8%) were common to the three extraction media and only a total of 40 ions (3.2%) were found to be medium specific. MWSF showed the best extraction yield with 97.4% of the total extractable *m/z* ions (N-IDY and Gplus-IDY MWSF had similar extraction yields with 85.4% and 89% respectively, data not shown). The polarity of the model wine appears to lead to a better solubilization of IDY compounds than water and methanol alone. Based on this result, G-IDY, Gplus-IDY and N-IDY MWSFs were compared in order to characterise the diversty of IDY extractible compounds. For all conditions, yeast derivatives were inactivated by short term heating before being dried and sealed hermetically for storage. In that respect, compounds potentially released by IDY are a combination of bio-accumulated metabolites and bio-transformed compounds related to the production process. Since the inactivation and drying process were identical for the three IDYs, it can be assumed that the major contribution to the diversity could be mainly attributed to the bio-process.

As shown in Figure 2B, 37.1% of the overall 1674 extractable ions were common to each IDY and only 1.8%, 3.9% and 11.7% of the ions were unique to G-IDY, N-IDY and Gplus-IDY, respectively. We also observed that N-IDY and G-IDY, obtained from the same yeast strain, shared more common ions (62.1%) than with Gplus-IDY (46.1% and 48.6% respectively). These results show that both the intracellular accumulation of glutathione and the yeast strain are key factors modifing the metabolic signatures of IDY soluble fractions, in agreement with existing literature (Allen et al., 2003; Brauer et al., 2006; Dikicioglu et al., 2012).

FIGURE 2

Network annotation of the *m/z* ions present in MWSF by NetCalc software allows access to the molecular formulas of 53% of the 1674 ions detected. The extensive chemical differences between G-IDY, Gplus-IDY and N-IDY MWSFs were clearly visible from the

histograms depicting the distribution of elemental compositions (CHO, CHON, CHOS, and CHONS), along with Van Krevelen diagrams of the (-)FT-ICR-MS derived molecular formulas (Figure 3). Figure 3A presents the 379 annotated *m/z* ions (42.7%) common to the three IDYs soluble fractions in model wine (MWSF). These ions could be considered as representative of extractable metabolites from IDYs whatever the strain or the production process. Common ions were found in different chemical spaces such as lipid-like, peptide-like and saccharide-like domains, which agrees with a glutathione accumulation bioprocess that preserves the yeast basic metabolism during the production.

FIGURE 3

Figure 3B, 3C and 3D show annotated masses unique to each MWSFs, colored according to their chemical compositions and sized according to their mass peak relative intensity. An overview of the Van Krevelen diagrams reveals significant differences between the samples in terms of number of unique formulas (already visible in Figure 2) and chemical families. N-IDY (Figure 3D) appeared much richer in unique CHO containing formulas (16) than G-IDY (3) and Gplus-IDY (0). These formulas are mainly in peptide-like and lipid-like domains, which could correspond to small chain fatty acids for example. In contrast, Gplus-IDY (Figure 3B) was characterized by a significantly higher number of unique CHONS containing formulas compared to G-IDY and N-IDY (36 against 3 and 1, respectively). These formulas, mainly located in the peptide-like domain could correspond to peptides with sulfur-containing amino acid residues, such as methionine and cysteine. The high diversity of sulfhydryl containing compounds (-SH group) could explain the relative activity of these products against oxidation, as it is known than peptides and thiols could have antioxidant property in wine (Elias et al., 2008; Nikolantonaki et al., 2010, 2014). It is remarkable to note how the glutathione enrichment process, which is designed to accumulate intracellular glutathione, is

actually accompanied by an overall increase of the CHONS/CHO ratio when going from N-IDY to Gplus-IDY (Figure 3E), with G-IDY potentially releasing 3 times more CHONS compounds than N-IDY, and Gplus-IDY releasing more than 10 times more compounds than N-IDY. With a moderate hypothesis of 3 isomers per (-)FT-ICR-MS ion, these results show altogether that Gplus-IDYs would be discriminated by more than 100 different N,S-containing compounds, compared to G-IDY and N-IDY, thus providing an unprecedented molecular representation of the actual metabolic response of glutathione enrichment. The relatively low number of unique compounds released from G-IDY is not surprising since it is obtained from the same strain as N-IDY, and it follows the same bio-process as Gplus-IDY, thus most of the released compounds are likely shared with at least one other IDY. Although it was not the aim of this study, it is further interesting to note the strain-dependency of the glutathione enrichment process, with Gplus-IDY releasing nearly 4 times more CHONS compounds than G-IDY while the released glutathione is increased by 2.

3.3. Impact of GSH enrichment process on IDYs peptides diversity

The presence of cysteine in the growth medium during IDY GSH accumulation processing at industrial scale (Li et al., 2004), modifies the global metabolism of sulfur amino acids and leads to over representation of sulfur-containing metabolites (Thomas & Surdin-Kerjan, 1997). As the Van Krevelen diagrams highlight the increasing diversity of CHON and CHONS containing compounds along with the enrichment process, this diversity could be putatively attributed to peptides containing cysteine or methionine residues. Amongst the 1674 *m/z* submitted to the OligoNet webserver, 193 were annotated as potential peptides (from 2 to 5 residues) with an error below 1ppm (Supplementary information 4). Within the 193 annotated ions, 132 have a Multiple Amino Acids Combination (MAAC) and 61 a Unique Amino Acids Combination (UAAC) (Figure 4A). Most of the peptides (144 *m/z*) are

common to at least two out of three IDYs, whereas Gplus-IDY presents the greatest diversity with 40 peptides against 7 and 2 for G-IDY and N-IDY, respectively. (Figure 4B). Amongst the UAAC, 26 out of 65 contain a cysteinyl residue. These unambiguous annotations of peptides allowed all possible connections between these peptides to be determined (Supplementary information 5). The Gplus-IDY clearly released more unique peptides and more peptides with a cysteinyl residue. Nevertheless, most of the UAAC are shared between the IDYs (regardless of their relative concentrations). The global similarity between our samples analyzed by (-)FT-ICR-MS allowed us to compare the absolute intensity between samples providing an indication of the abundance of each compound released. Figure 4C reveals that within the 61 UAAC released by the IDY, Gplus-IDY released 28 peptides significantly more intense than G- and N-IDY (3 peptides and 1 peptides respectively). These results are in accordance with the Van Krevelen diagram (Figure 3B) showing a higher diversity of compounds in the peptide-like domain for Gplus-IDY.

FIGURE 4

In addition to the peptides enrichment, other metabolites could be impacted by the bio-process. (-)FT-ICR-MS enables to have access to the elemental formulas of detected ions and thus to acquire instantaneous metabolic fingerprints of what can be released by IDYs. Since a single CHONS elemental formula can be associated with numerous compounds, (especially for high *m/z* ions) the combination with separative UHPLC-Q-ToF-MS and UHPLC-Q-ToF-MS S/MS methods was used to access structural and quantitative information about these molecular markers (Roullier-Gall et al., 2014). The highest resolution of the (-)FT-ICR-MS (600,000 against 20,000 for UHPLC-Q-ToF-MS at *m/z* 306) was used to annotate UHPLC-Q-ToF-MS peaks which could be aligned with (-)FT-ICR-MS peaks, using an in-house designed alignment script. Up to 128 *m/z* peaks of the UHPLC-Q-ToF-MS spectra where found to match (-)FT-ICR-MS peaks (with an absolute error lower than 2 ppm)

(Supplementary information 6) . Alignment was done on the basis of the similarity of *m/z* without consideration of the retention time, only for the negative mode of the UHPLC-Q-ToF-MS . The aim was to have both an unambiguous annotation of UHPLC-Q-ToF-MS ions with the ultrahigh resolution of (-)FT-ICR-MS, and quantitative information from UHPLC-Q-ToF-MS. Ions present UHPLC-Q-ToF-MS data but not found in (-)FT-ICR-MS data (Figure 4B) were likely molecules easily suppressed in direct infusion with ESI, showing the added value of using chromatographic separation before MS analysis (Roullier-Gall et al., 2014).

Keeping in mind the formula annotation of *m/z* ions with the (-)FT-ICR-MS data, the fragmentation of 16 important ions (issued from positive and negative ionization mode) enabled to have access to molecular structural information. Fragments were submitted to metabolomic databases, and annotation of the parent's ions are summarized in Table 1. Following the new prescriptions of Sumner and collaborators, the identification point (which gives the identification confidence level) of each metabolite is 5.5 (High resolution retention time, accurate mass of parent ion, molecular formula based upon accurate m/z and isotope pattern and accurate tandem mass spectrum) (Sumner et al., 2014). Most of these compounds were already described in yeast metabolic pathways, but never so far as compounds which could be potentially extracted from IDY in winemaking conditions. Most interestingly, glutathione and its precursor (glutamyl-cysteine) were found in the three extracts, but consistently with the enrichment process, *i.e.* with a relative abundance following the Gplus > G > N trend. In contrast, lysine-leucine and arginine-leucine dipeptides appeared as GPlus-IDY markers, whereas homocitric acid appeared as N-IDY marker. Amino acids (glutamate, tyrosine, phenylalanine), which have been extensively studied in IDY (Pozo-Bayón et al., 2009) were examples of contrasted trends with relative concentrations that did not appear to be directly correlated to the GSH accumulation process. Similarly, methyl-thioadenosine, a precursors of adenosylmethionine which is a sulfur and nitrogen stock molecule in poor

medium (Shapiro & Schlenk, 1980), and thus a potential fermentation enhancer already putatively annotated in IDYs (Rodriguez-Bencomo et al., 2014) were identify in the three samples. Weak organic acids like citric acid have been described for their sensory impact (fresh notes), whereas homocitric acid and pipecolic are related to the lysine metabolism in yeast (He, 2006; Tucci & Ceci, 1972), but not yet described in IDYs. Finally, the pantothenic acid, which exhibits a promoting effect on yeast growth (Richards, 1936) is much more present in N-IDY than in G-IDY and Gplus-IDY. Adenosine and arginine-leucine were recently shown to possibly promote bacteria growth (Liu et al., 2016; Liu et al., 2017) and thus facilitate the malolactic fermentation. Whereas Adenosine are abundant in the three IDYs, the dipeptide Arg-Leu is specific to Gplus-IDY and almost absent in the other IDYs. Such structural identifications provide a good overview of the richness and the diversity of compounds released by IDYs, and it also highlights the yet unknown potential contribution of IDYs during fermentation.

TABLE 1

Most of the ions detected by (-)FT-ICR-MS and UHPLC-Q-ToF-MS are difficult to isolate and fragment, which implies that most of the compounds present in the MWSFs are still largely unknown. Supplementary Information 7 gives the list of NetCalc annotated (-)FT-ICR-MS peaks found in the database, with the relative intensity of each ion and these possible database ID with an error lower than 2ppm. In this way we can have a quick overview of specific and common compounds from each IDY and appreciate how the medium is modified by using specific IDY.

4. Conclusion

In this work, the soluble fraction that can be extracted from three inactive dry yeasts by model wine, were characterized by a combination of Gel Permeation chromatography (GPC), (-)FT-ICR-MS and UHPLC-Q-ToF-MS in order to provide a comprehensive picture

of the diversity of potentially active compounds associated with the glutathione accumulation process. To that purpose, the extract of non-enriched IDYs (N-IDY) was compared to extracts of an GSH-rich IDY from the same strain (G-IDY) and an even more GSH-rich IDY, but from a different strain (Gplus-IDY). Consistently with the expected GSH accumulation process, Gplus-IDY exhibited higher amounts of extractable glutathione (and its glutamyl-cysteine precursor) than G-IDY, which in turn appeared richer than N-IDY. Moreover, the increase in peptides containing cysteinyl residues in Gplus-IDY shows than the glutathione accumulation bio-process also impacts the peptidome of the yeast. Modulation of the GSH pathway leads to a global modification of cysteine incorporation and thus could have important implications in wine making.

Our metabolomic approach provided a comprehensive molecular picture of the detailed impact of the glutathione accumulation process. It further revealed how the yeast strain can modulate the extent of the accumulation process, with the annotation of more than hundred N,S-containing potential active compounds for Gplus-IDYs, most of them being unknown yet. Altogether, our results shed important light on the potential activity of IDYs on musts and wines, in terms of organoleptic and/or stability properties.

ACKNOWLEDGEMENTS

The authors acknowledge the Regional Council of Bourgogne – Franche-Comté, the “Fonds Européen de DEveloppement Régional (FEDER)” and Lallemand SAS (31, Blagnac), for financial support. They also would like to thank Dr. Eveline Bartowsky for a careful reading of the manuscript by a native English speaker.

Conflicts of interest

The authors wish to confirm that there are no conflicts of interest associated with this publication.

Abbreviations used

IDY, inactivated dry yeast; GSH, glutathione; MS, mass spectrometry; WSF, water soluble fraction; MWSF, model wine soluble fraction; MSF, methanol soluble fraction; GPC, gel permeation chromatography; HPLC, high pressure liquid chromatography; DAD, diode array detector; LMW, low molecular weight; UHPLC-Q-ToF-MS , Ultra-High-Performance Liquid chromatography triple quadrupole time of flight mass spectrometry; RP-LC, reversed phase liquid chromatography; (-)FT-ICR-MS, Negative mode Fourier-transform ion-cyclotron-resonance mass spectrometry; S/N, Signal/Noise; kDa, kilo Dalton; MAAC, Multiple Amino Acid Combination; UAAC, Unique Amino Acid Combination; CHO, Carbon-Hydrogen-Oxygen; CHON, Carbon-Hydrogen-Oxygen-Nitrogen; CHONS, Carbon-Hydrogen-Oxygen-Nitrogen-Sulfur

REFERENCES

Allen, J., Davey, H. M., Broadhurst, D., Heald, J. K., Rowland, J. J., Oliver, S. G., & Kell, D. B. (2003). High-throughput classification of yeast mutants for functional genomics using metabolic footprinting. *Nature Biotechnology*, *21*(6), 692–696.

Andújar-Ortiz, I., Pozo-Bayón, M. Á., Garrido, I., Martin-Álvarez, P. J., Bartolomé, B., & Moreno-Arribas, M. V. (2012). Effect of using glutathione-enriched inactive dry yeast preparations on the phenolic composition of rosé grenache wines during winemaking. *Journal International Des Sciences de La Vigne et Du Vin*, *46*(3), 241–251.

Antoce, A. O., Badea, G. A., & Cojocaru, G. A. (2016). Effects of Glutathione and Ascorbic Acid Addition on the CIELab Chromatic Characteristics of Muscat Ottonel Wines.

Agriculture and Agricultural Science Procedia, *10*, 206–214.

Brauer, M. J., Yuan, J., Bennett, B. D., Lu, W., Kimball, E., Botstein, D., & Rabinowitz, J. D. (2006). Conservation of the metabolomic response to starvation across two divergent microbes. *Proceedings of the National Academy of Sciences*, *103*(51), 19302–19307.

Brockman, S. A., Roden, E. V., & Hegeman, A. D. (2018). Van Krevelen diagram visualization of high resolution-mass spectrometry metabolomics data with OpenVanKrevelen. *Metabolomics*, *14*(4), 48.

Chertov, O., Biragyn, A., Kwak, L. W., Simpson, J. T., Boronina, T., Hoang, V. M., Fisher, R. J. (2004). Organic solvent extraction of proteins and peptides from serum as an effective sample preparation for detection and identification of biomarkers by mass spectrometry. *Proteomics*, *4*(4), 1195–1203.

Coelho, C., Parot, J., Gonsior, M., Nikolantonaki, M., Schmitt-Kopplin, P., Parlanti, E., & Gougeon, R. D. (2017). Asymmetrical flow field-flow fractionation of white wine chromophoric colloidal matter. *Analytical and Bioanalytical Chemistry*, *409*(10), 2757–2766.

Dikicioglu, D., Dunn, W. B., Kell, D. B., Kirdar, B., & Oliver, S. G. (2012). Short- and long-term dynamic responses of the metabolic network and gene expression in yeast to a transient change in the nutrient environment. *Molecular BioSystems*, *8*(6), 1760.

Elias, R. J., Kellerby, S. S., & Decker, E. A. (2008). Antioxidant Activity of Proteins and Peptides. *Critical Reviews in Food Science and Nutrition*, *48*(5), 430–441.

Elskens, M. T., Jaspers, C. J., & Penninckx, M. J. (1991). Glutathione as an endogenous sulphur source in the yeast Saccharomyces cerevisiae. *Journal of General Microbiology*, *137*, 637–644.

Escot, S., Feuillat, M., Dulau, L., & Charpentier, C. (2001). Release of polysaccharides by yeasts and the influence of released polysaccharides on colour stability and wine

astringency. *Australian Journal of Grape and Wine Research*, *7*(3), 153–159.

Gougeon, R. D., Lucio, M., Frommberger, M., Peyron, D., Chassagne, D., Alexandre, H., Schmitt-Kopplin, P. (2009). The chemodiversity of wines can reveal a metabologeography expression of cooperage oak wood. *Proceedings of the National Academy of Sciences*, *106*(23), 9174–9179.

Guadalupe, Z., & Ayestarán, B. (2008). Effect of commercial mannoprotein addition on polysaccharide, polyphenolic, and color composition in red wines. *Journal of Agricultural and Food Chemistry*, *56*(19), 9022–9029.

He, M. (2006). Pipecolic acid in microbes: Biosynthetic routes and enzymes. *Journal of Industrial Microbiology and Biotechnology*, *33*(6), 401–407.

Jaehrig, S. C., Rohn, S., Kroh, L. W., Wildenauer, F. X., Lisdat, F., Fleischer, L. G., & Kurz, T. (2008). Antioxidative activity of (1→3), (1→6)-β-d-glucan from Saccharomyces cerevisiae grown on different media. *LWT - Food Science and Technology*, *41*(5), 868–877.

Jaehrig, S., & Rohn, S. (2007). In Vitro Potential Antioxidant Activity of (1→3), (1→6)-β-d-glucan and Protein Fractions from Saccharomyces cerevisiae Cell Walls. *Journal of Agricultural and Food Chemestry*, *55*(12), 4710–4716.

Kim, S., Kramer, R. W., & Hatcher, P. G. (2003). Graphical Method for Analysis of Ultrahigh-Resolution Broadband Mass Spectra of Natural Organic Matter, the Van Krevelen Diagram. *Analytical Chemistry*, *75*(20), 5336–5344.

Kritzinger, E. C., Bauer, F. F., & Du Toit, W. J. (2013). Role of glutathione in winemaking: A review. *Journal of Agricultural and Food Chemistry*, *61*(2), 269–277.

Li, Y., Wei, G., & Chen, J. (2004, October). Glutathione: A review on biotechnological production. *Applied Microbiology and Biotechnology*.

Liu, Y., Forcisi, S., Harir, M., Deleris-Bou, M., Krieger-Weber, S., Lucio, M., Alexandre, H.

(2016). New molecular evidence of wine yeast-bacteria interaction unraveled by non-targeted exometabolomic profiling. *Metabolomics*, *12*(4).

Liu, Y., Forcisi, S., Lucio, M., Harir, M., Bahut, F., Deleris-Bou, M., Schmitt-Kopplin, P. (2017). Digging into the low molecular weight peptidome with the OligoNet web server. *Scientific Reports*, *7*(1), 11692.

Liu, Y., Rousseaux, S., Tourdot-Maréchal, R., Sadoudi, M., Gougeon, R., Schmitt-Kopplin, P., & Alexandre, H. (2017). Wine microbiome: A dynamic world of microbial interactions. *Critical Reviews in Food Science and Nutrition*, *57*(4), 856–873.

Lucio, M. (2009). *Datamining metabolomics: the convergence point of non-target approach and statistical investigation*. Fakultät Wissenschaftszentrum Weihenstephan.

Nikolantonaki, M., Chichuc, I., Teissedre, P.-L., & Darriet, P. (2010). Reactivity of volatile thiols with polyphenols in a wine-model medium: Impact of oxygen, iron, and sulfur dioxide. *Analytica Chimica Acta*, *660*, 102–109.

Nikolantonaki, M., Julien, P., Coelho, C., Roullier-Gall, C., Ballester, J., Schmitt-Kopplin, P., & Gougeon, R. D. (2018). Impact of Glutathione on Wines Oxidative Stability: A Combined Sensory and Metabolomic Study. *Frontiers in Chemistry*, *6*(June), 1–9.

Nikolantonaki, M., Magiatis, P., & Waterhouse, A. L. (2014). Measuring protection of aromatic wine thiols from oxidation by competitive reactions vs wine preservatives with ortho-quinones. *Food Chemistry*, *163*, 61–67.

Nisamedtinov, I., Kevvai, K., Orumets, K., Arike, L., Sarand, I., Korhola, M., & Paalme, T. (2011). Metabolic changes underlying the higher accumulation of glutathione in Saccharomyces cerevisiae mutants. *Applied Microbiology and Biotechnology*, *89*(4), 1029–1037.

Pozo-Bayón, M. Á., Andujar-Ortiz, I., Alcaide-Hidalgo, J. M., Martín-Álvarez, P. J., & Moreno-Arribas, M. V. (2009). Characterization of commercial inactive dry yeast

preparations for enological use based on their ability to release soluble compounds and their behavior toward aroma compounds in model wines. *Journal of Agricultural and Food Chemistry*, *57*(22), 10784–10792.

Ramirez-Gaona, M., Marcu, A., Pon, A., Guo, A. C., Sajed, T., Wishart, N. A., Wishart, D. S. (2017). YMDB 2.0: a significantly expanded version of the yeast metabolome database. *Nucleic Acids Research*, *45*.

Richards, O. W. (1936). The stimulation of yeast proliferation by pantothenic acid. *Journal of Biological Chemistry*, *113*(4360), 531–536.

Rodriguez-Bencomo, J. J., Andujar-Ortiz, I., Moreno-Arribas, M. V., Sima, C., Gonzalez, J., Chana, A., Pozo-Bayon, M. A. (2014). Impact of glutathione-enriched inactive dry yeast preparations on the stability of terpenes during model wine aging. *Journal of Agricultural and Food Chemistry*, *62*(6), 1373–1383.

Roullier-Gall, C., Hemmler, D., Gonsior, M., Li, Y., Nikolantonaki, M., Aron, A., Schmitt-Kopplin, P. (2017). Sulfites and the wine metabolome. *Food Chemistry*, *237*, 106–113.

Roullier-Gall, C., Witting, M., Gougeon, R. D., & Schmitt-Kopplin, P. (2014). High precision mass measurements for wine metabolomics. *Frontiers in Chemistry*, *2*, 102.

Roullier-gall, C., Witting, M., Tziotis, D., Ruf, A., & Gougeon, R. D. (2015). Integrating analytical resolutions in non-targeted wine metabolomics. *Tetrahedron*, *71*(20), 2983–2990.

Shapiro, S. K., & Schlenk, F. (1980). Conversion of 5'-methylthioadenosine into S-adenosylmethionine by yeast cells. *Biochimica et Biophysica Acta*, *633*(2), 176–80.

Stoscheck, C. M. (1990). Quantitation of protein. *Methods in Enzymology*, *182*(1987), 50–68.

Suhre, K., & Schmitt-Kopplin, P. (2008). MassTRIX: mass translator into pathways. *Nucleic Acids Research Web Server*, *36*, 481–484.

Sumner, L. W., Lei, Z., Nikolau, B. J., Saito, K., Roessner, U., & Trengove, R. (2014).

Proposed quantitative and alphanumeric metabolite identification metrics. *Metabolomics*. Springer US.

Thomas, D., & Surdin-Kerjan, Y. (1997). Metabolism of sulfur amino acids in Saccharomyces cerevisiae. *Microbiology and Molecular Biology Reviews : MMBR*, *61*(4), 503–32.

Tucci, A. F., & Ceci, L. N. (1972). Homocitrate synthase from yeast. *Archives of Biochemistry and Biophysics*, *153*(2), 742–750.

Tziotis, D., Hertkorn, N., & Schmitt-Kopplin, P. (2011). Letter: Kendrick-analogous network visualisation of ion cyclotron resonance Fourier transform mass spectra: improved options for the assignment of elemental compositions and the classification of organic molecular complexity. *European Journal of Mass Spectrometry*, *17*(4), 415.

Webber, V., Dutra, S. V., Spinelli, F. R., Carnieli, G. J., Cardozo, A., & Vanderlinde, R. (2016). Effect of glutathione during bottle storage of sparkling wine. *Food Chemistry*.

Wen, S., Zhang, T., & Tan, T. (2004). Utilization of amino acids to enhance glutathione production in Saccharomyces cerevisiae. *Enzyme and Microbial Technology*, *35*(6–7), 501–507.

Figure and Table Captions

Figure 1: Gel permeation chromatograms of model wine soluble fractions (MWSF) of G-IDY (red), Gplus-IDY (green) and N-IDY (black) with fluorescence detection (EX/EM = 280/350 nm). Dotted lines indicate the calibration areas based on standard compounds.

Figure 2: Venn diagrams presenting the total counts of detected ions by (-)FT-ICR-MS, with percentages in brackets. (A) Extraction yield for the specific G-IDY in the three extraction media, and (B) unique and common ions to the model wine soluble fractions of N-IDY, G-IDY and Gplus-IDY.

Figure 3: Van Krevelen representation of annotated masses from (-)FT-ICR-MS analyses of the MWSFs (Model Wine Soluble Fraction) of Gplus-IDY, G-IDY and N-IDY. (A) masses shared by Gplus-IDY, G-IDY and N-IDY MWSFs. (B) Specific *m/z* ions to Gplus-IDY , (C) specific *m/z* ions to G-IDY, and (D) specific *m/z* ions to N-IDY. In B, C and D common *m/z* ions were depicted in grey. Van Krevelen plots were coloured according to molecular classes i.e CHO (blue), CHOS (green), CHON (orange), CHONS (red). Bubble sizes correspond to the triplicate averaged relative intensities of mass peaks. Bar histograms indicate the number (and corresponding percentage at the bar-top) of molecular formulae presented in the Van Krevelen diagrams. (E) Relative abundance of CHONS against CHO for the three MWSFs. For each IDY, the total number of annotated masses corresponding to CHO and CHONS were used to calculate this ratio.

Figure 4: 193 potential peptides annotation, out of the 1674 *m/z* from (-)FT-ICR-MS submitted to the OligoNet webserver. (A) Annotations correspond to 142 Multiple Amino Acid Combination (MAAC, with 89 and 43 with and without cysteinyl residue respectively) and 61 Unique Amino Acid Combination (UAAC, with 26 and 35 with and without cysteinyl residue respectively). (B) Within the 193 potential peptides N-IDY (red), G-IDY (blue) and Gplus-IDY (green) released 2, 7 and 40 unique *m/z* attributed to peptides, respectively. The 144 remaining potential peptides are shared (grey) by at least 2 IDYs. (C) Amongst the 61 UAAC, 28 are significantly more released by Gplus-IDY, in contrast only 3 and 1 are more abundant using G- or N-IDY respectively (p-value < 0.05).

630 **Table 1**: Metabolites fragmented by UHPLC-Q-ToF-MS/MS in the MWSF for the three
631 IDYs, and their corresponding chemical family. Main fragments used to identify features
632 from databases are listed in the discriminant fragments column allowing a high confidence
633 level. Relative abundance of metabolites between IDYs is expressed as percentage of the
634 biggest area. The identification is the combination of composition elucidation by (-)FT-ICR-
635 MS (when available) and structural elucidation by UHPLC-Q-ToF-MS /MS.
636

m/z Adduct	Ret. time (min)	Collision energy (eV)	Discriminant Fragments	Annotation [M]	Error (ppm)	Area (%) N-IDY	Area (%) G-IDY	Area (%) Gplus-IDY	Identified metabolite	Database ID
130.0863 [M+H]+	0.7	30	84.0808	$C_6H_{11}NO_2$	0.35	**100**	**43**	**41**	*Pipecolic acid*	C00408 (KEGG)
148.0601 [M+H]+	0.6	15	84.0447;130.0497	$C_5H_9NO_4$	-2.03	**100**	**78**	**53**	*Glutamic acid*	C00025 (KEGG)
165.0548 [M+H]+	0.7	10	147.0442;119.0492 ;91.0544	$C_9H_8O_3$	1.08	**47**	**30**	**100**	*Coumaric acid*	C12621/ C00811 (KEGG)
166.0861 [M+H]+	1.0	15	166.0862;120.0806 ;131.0490	$C_9H_{11}NO_2$	-1.20	**44**	**36**	**100**	*Phenylalanine*	C00079 (KEGG)
179.0485 [M+H]+	0.7	10	162.0222;144.0116 ;116.0164	$C_5H_{10}N_2O_3S$	0.06	**36**	**91**	**100**	*Cysteinyl-glycine*	C01419 (KEGG)
182.0811 [M+H]+	0.7	15	136.0757;123.0438 ;147.0442	$C_9H_{11}NO_3$	-0.55	**71**	**43**	**100**	*Tyrosine*	C00082 (KEGG)
191.0199 [M-H]-	0.7	15	173.0095;129.0197 ;111.0094	$C_6H_8O_7$	1.05	**100**	**37**	**17**	*Citric acid*	C00158 (KEGG)
205.0355 [M-H]-	0.8	15	143.0352;125.0248	$C_7H_{10}O_7$	0.49	**100**	**<1**	**<1**	*Homocitric acid*	C05662 (KEGG)
218.1037 [M-H]-	1.1	15	146.082	$C_9H_{17}NO_5$	1.38	**100**	**63**	**73**	*Pantothenic acid*	C00864 (KEGG)
251.0693 [M+H]+	0.7	15	122.0269;130.0497 ;188.0373	$C_8H_{14}N_2O_5S$	-1.19	**19**	**71**	**100**	*Glutamyl-cysteine*	C00669 (KEGG)
258.11 [M+H]+	0.6	20	184.0735;104.1070	$C_8H_{20}NO_6P$	-0.39	**18**	**23**	**100**	*Glycerophosphocholine*	C00670 (KEGG)
260.1969 [M+H]+	0.8	30	147.1132;129.1025 ;84.0810	$C_{12}H_{25}N_3O_3$	0.12	**<1**	**<1**	**100**	*Leucyl-lysine*	HMDB28912 (HMDB)
268.1037 [M+H]+	0.7	15	119.0353;136.0617	$C_{10}H_{13}N_5O_4$	-1.12	**92**	**100**	**94**	*Adenosine*	C00212 (KEGG)
288.2030 [M+H]+	0.8	20	271.1763;175.1187	$C_{12}H_{25}N_5O_3$	-0.06	**<1**	**<1**	**100**	*Leucyl-arginine*	HMDB28923 (HMDB)
298.0970 [M+H]+	1.3	15	136.0616;145.0320	$C_{11}H_{15}N_5O_3S$	0.67	**74**	**100**	**85**	*Methyl-thioadenosine*	C00170 (KEGG)
306.0763 [M-H]-	0.7	15	272.0890;143.0464 ;210.0882	$C_{10}H_{17}N_3O_6S$	-0.65	**33**	**89**	**100**	*Glutathione*	C00051 (KEGG)

637

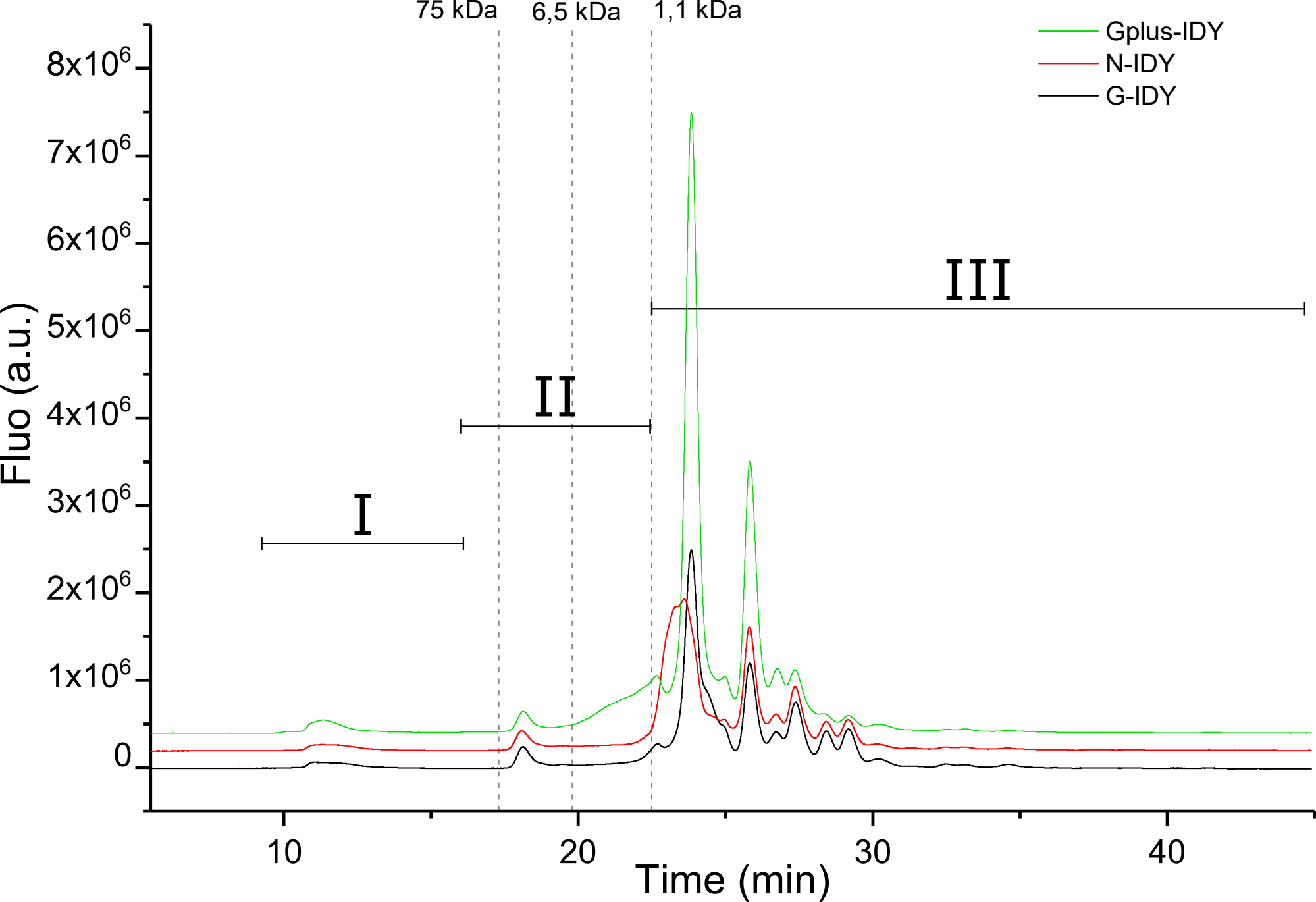
75 kDa
6,5 kDa
1,1 kDa
Gplus-IDY
N-IDY
G-IDY
I
II
III
Fluo (a.u.)
8x10^6
7x10^6
6x10^6
5x10^6
4x10^6
3x10^6
2x10^6
1x10^6
0
10
20
30
40
Time (min)

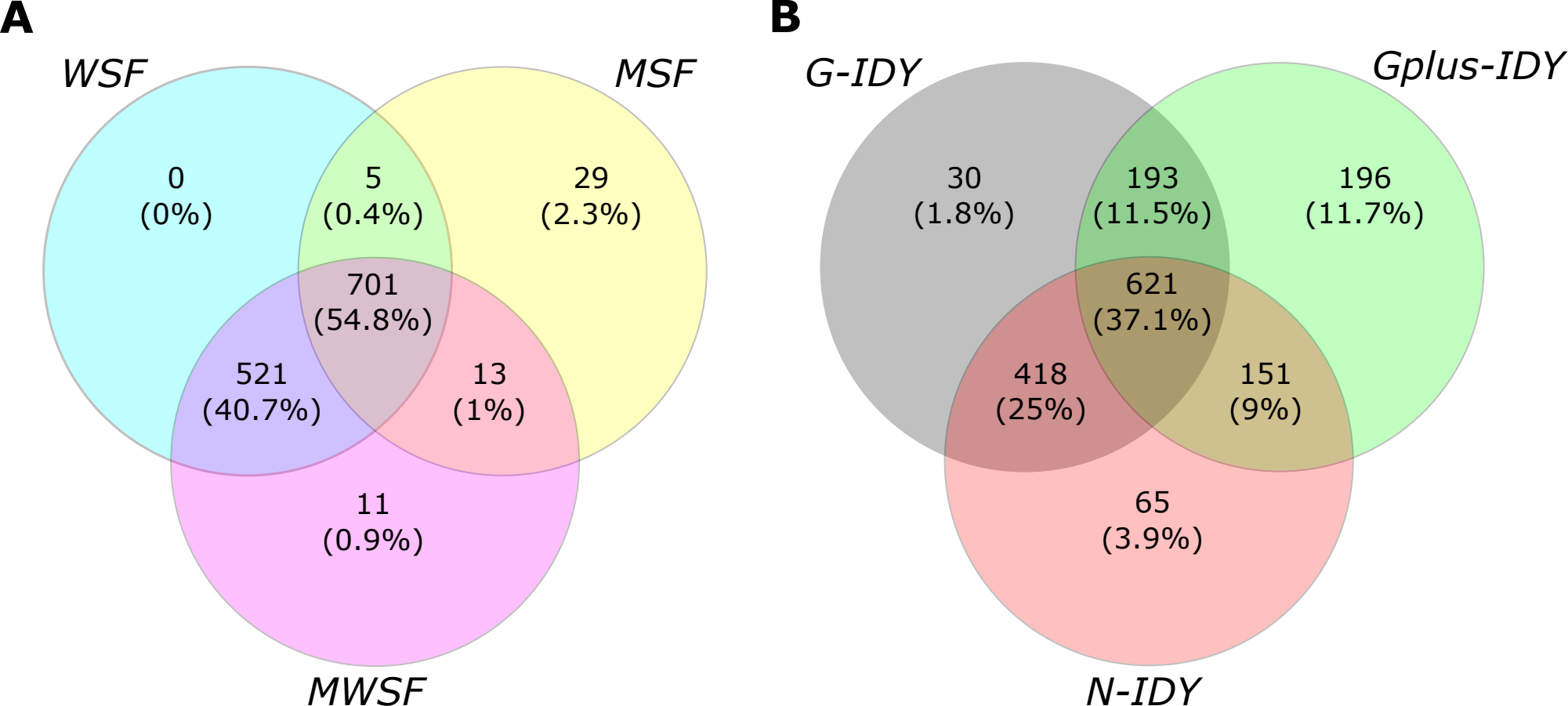
A
WSF
MSF
MWSF
0
(0%)
5
(0.4%)
29
(2.3%)
701
(54.8%)
521
(40.7%)
13
(1%)
11
(0.9%)
B
G-IDY
Gplus-IDY
N-IDY
30
(1.8%)
193
(11.5%)
196
(11.7%)
621
(37.1%)
418
(25%)
151
(9%)
65
(3.9%)

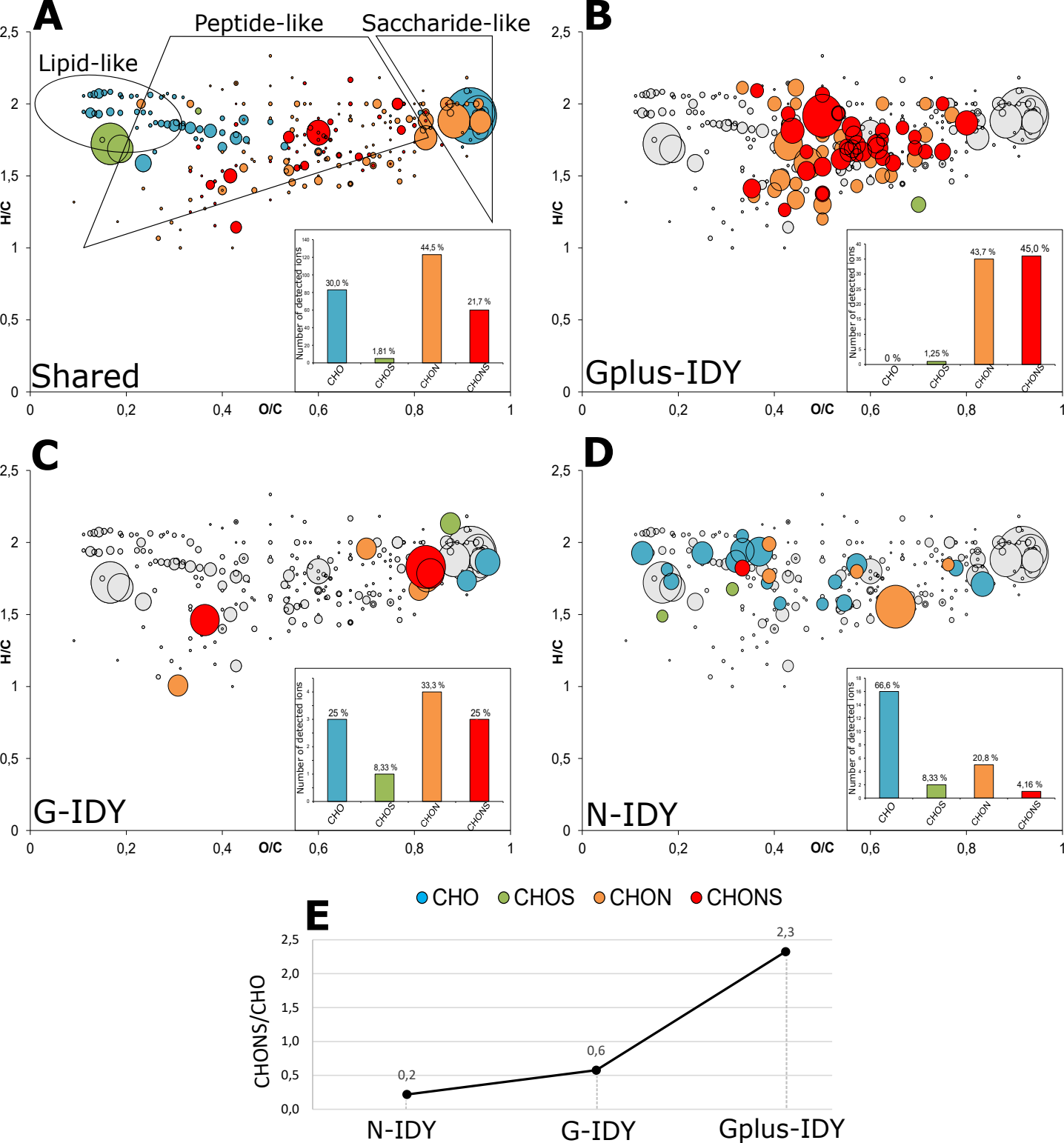
A
Peptide-like
Saccharide-like
Lipid-like
Shared
B
Gplus-IDY
C
G-IDY
D
N-IDY
H/C
O/C
Number of detected ions
CHO
CHOS
CHON
CHONS
30,0 %
1,81 %
44,5 %
21,7 %
0 %
1,25 %
43,7 %
45,0 %
25 %
8,33 %
33,3 %
25 %
66,6 %
8,33 %
20,8 %
4,16 %
E
CHONS/CHO
0,2
0,6
2,3
N-IDY
G-IDY
Gplus-IDY

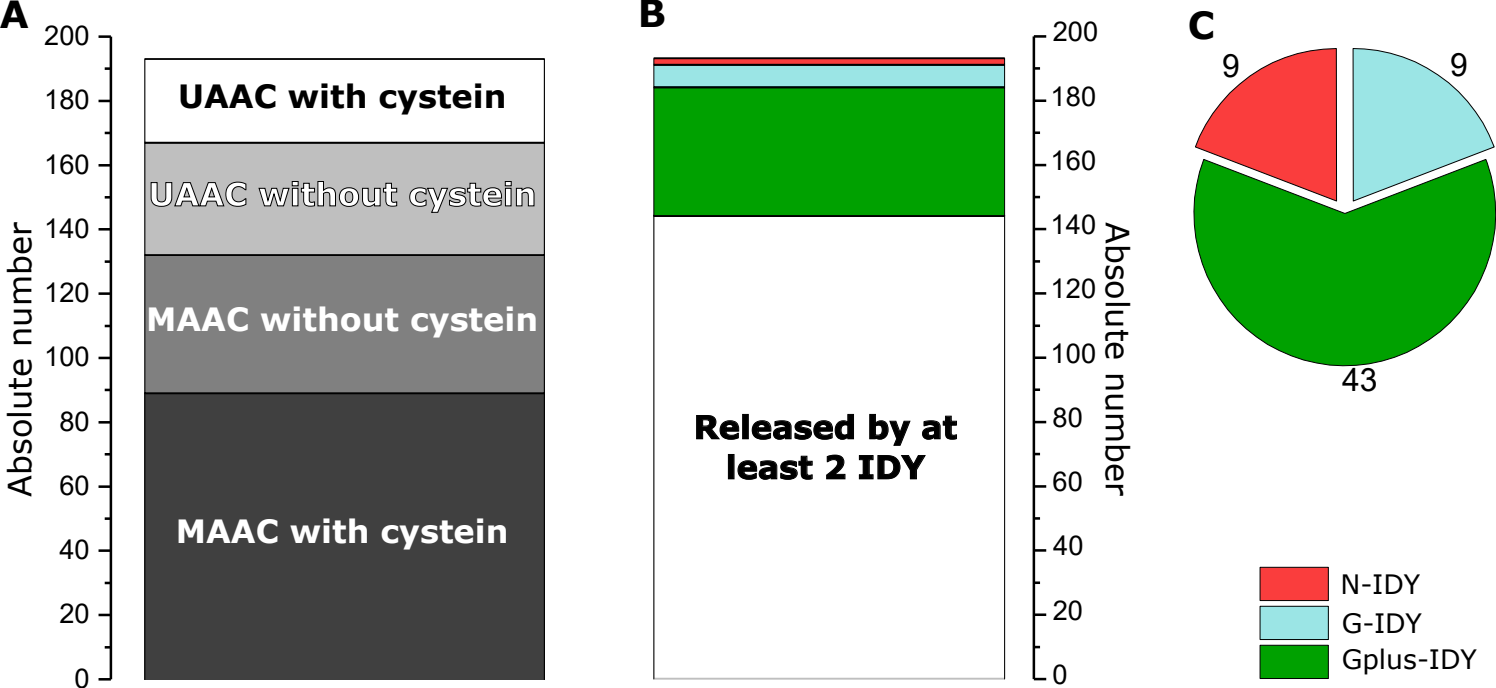
A
Absolute number
200
180
160
140
120
100
80
60
40
20
0
UAAC with cystein
UAAC without cystein
MAAC without cystein
MAAC with cystein
B
Released by at least 2 IDY
Absolute number
C
9
9
43
N-IDY
G-IDY
Gplus-IDY

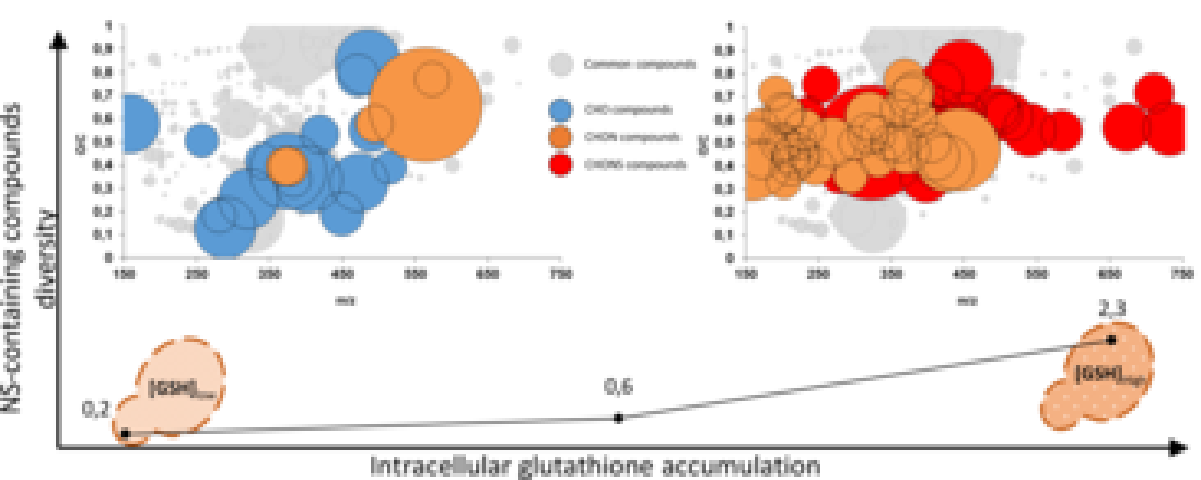
Common compounds
CHO compounds
CHON compounds
CHONS compounds
sc
m/z
NS-containing compounds diversity
Intracellular glutathione accumulation
0,2
0,6
2,3
[GSH]low
[GSH]high